Journal of Basic and Environmental Sciences, 7 (2020) 1-12

ISSN

Online: 2356-6388

Print: 2536-9202

Research paper **Open Access**

Characterization and Application of Olive Stones Activated Carbon for Uranium (VI) Sorption from Wet-process phosphoric acid: Kinetic, equilibrium and thermodynamic studies

Walid M. Youssef
Nuclear Materials Authority, P.O. Box 530, El-Maadi, Cairo, Egypt
E-mail: m.walid_nma@yahoo.com

Abstract

In this work, uranium adsorption from Egyptian phosphoric acid onto chemical modified Olive Stones has been studied by two methods (H_3PO_4 and $ZnCl_2$) at 800ºC was used to carbonized. The relevant factors affecting uranium adsorption onto our Olive Stones Activated Carbon adsorbent were studied. These factors involved phosphoric acid concentration, the contact time, adsorbent weight, initial uranium concentration and the temperature were investigated. The theoretical capacity of Olive Stones Activated Carbon adsorbent is about (47.8, 46.08) mg/g for O.S-H_3PO_4, O.S-$ZnCl_2$ respectively. The optimum adsorption conditions were choiced in two methods and P_2O_5 ineffective by these conditions. The sorption process of uranium U(VI) follow Langmuir isotherm model with pseudo-second order mechanism and exothermic nature and spontaneous process according to studying (enthalpy change, entropy change and Gibbs free energy change). More Than 80 % of the loaded uranium amount on the Olive Stones Activated Carbon adsorbent has been eluted using 0.1 M HNO_3 as an efficient eluent.

Keywords: Activated Carbon, Olive stone, uranium U(VI), H_3PO_4, $ZnCl_2$, Sorption.

Received; 20 Aug. 2019, Revised form; 17 Oct. 2019, Accepted; 17 Oct. 2019, Available online 1 Jan. 2020.

1. Introduction

Uranium is a naturally occurring radioactive material (NORM) that could be found in our environment. In addition to the naturally occurring amount, industries such as mining, ore processing, fossil fuel extraction, commercial aviation, and use of uranium-containing phosphate fertilizers, do increase the amount of uranium in the environment. Because of its radioactivity of naturally occurring uranium is only marginal, and chemotoxic, Uranium is considered as one of dangerous environmental waste [1, 2].

Phosphoric acid is one of the most important and useful mineral acids. Commercially, phosphoric acid is manufactured using different processes, the most commonly used are: thermal and wet-process. The wet-process involves reaction of phosphate rock with an acid (mainly sulfuric acid) [3]. Wet-process phosphoric acid (WPA) is an important unconventional source of uranium. The quantities of available uranium vary within a deposit and between different mineral fields (from 20 to 200 ppm). Considering the total amount of phosphate rock, uranium recovery from this resource is an alternative to uranium production from uranium ores [4]. Several methods have been investigated to remove uranium from WPA such as precipitation [5], ion-exchange [6], membrane separation [7], solid-liquid [8] and liquid-liquid extraction [9], Solvent-In-Pulp [10]

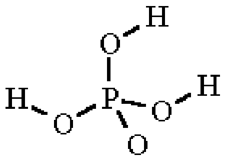

H_3PO_4 phosphoric acid

Among these techniques, the adsorption method using an efficient adsorbent has been considered most feasible. It has been shown that adsorption is not only a removal process, but it also allows enrichment and pre-concentration of uranium. The uptake of uranium on various solids such as activated carbon [11] montmorillonite [12], kaolinite [13], zeolite [14], titanium nanotubes [15]. Activated carbons are made from materials rich in carbon through carbonization and an activation process. A porous structure and its adsorption properties can be obtained in carbonaceous materials via either chemical or physical activation, and leading industrial materials due to its well-developed pore structure and adsorption properties [16-19]. Chemical activation involves the impregnation of the precursor material with a chemical activating agent followed under temperatures, nitrogen atmosphere, Zinc chloride ($ZnCl_2$), potassium hydroxide (KOH) and phosphoric acid (H_3PO_4) are widely used as chemical activating agents [20-23] .Olive stone used in this study, due to its high surface area, high adsorption capacity, microporous structure and special surface reactivity .It would add value to these agricultural commodities, help reduce the cost of waste disposal, and provide a potentially cheap alternative to the existing commercial carbons [24-26]. The preparation of activated carbon from olive stone using a base leaching or acid-washing process has not been well studied.

In view of the above, the current paper has focused on with the preparation of activated carbon from olive stone using chemical activation by H_3PO_4 and other method by $ZnCl_2$ then studying the factors affecting the sorption processes of U (VI) ions from Wet-process phosphoric acid (WPA). Equilibrium adsorption isotherms are analyzed to obtain the Langmuir and Freundlich constants.

2. Experimental Section

2.1. Materials and Reagents

All reagents used were of analytical reagent grade. Olive stone (O.S.) was obtained from Qaha for preserved food Co., uranyl acetate, crude high strength phosphoric acid under study was produced from Abu Zaabal Company for Fertilizer and Chemical Materials (AZFC), its chemical composition is given in (Table 1).

Table 1: Chemical analysis of crude high strength phosphoric acid produced from AZFC.

Component	Concentration
P_2O_5	≈ 44.0 %
Ca	0.44 %
SO_4^{--}	5.84 %
SiO_2	0.96 %
F	1.20 %
Fe	2.40 %
U	50 ppm

The green phosphoric acid was subjected to prior treatment process, as following; first cooling down to room temperature (25 ± 1ºC), then treated with clay for suspended solid particles removal, after that treating with granular charcoal in order to remove soluble organic matters and finally oxidation with hydrogen peroxide till EMF > 450 mv.

Thermostat shaker water bath having a temperature variation of ± 0.5°C used for batch equilibrium experiments was obtained from Joshi Scientific Corporation. Inductively coupled plasma optical emission spectrometer (Optima 2100DV, Perkin-Elmer) was used to determine uranium (VI) and P_2O_5. Whatman-42 grade filter paper was used for filtration and an oven of Meta-Lab, model MSI-66 was used to dry the sorbent beads.

2.2. Preparation of activated carbon:

Olive stone, as an agro-residue byproduct, was chosen as a precursor for the production of activated carbons by one-step chemical activation using two methods, first method 50% H_3PO_4. In each experiment 30 gm drying, crushed of olive stone was soaked in 50% phosphoric acid (BDH) [27-29]. The O.S mass was soaked in 150 mL of H_3PO_4 solution, slightly agitated to ensure penetration of the acid throughout, then the mixture was heated to 80 ºC for 1 h and left overnight at room temperature to help appropriate wetting and impregnation of the precursor. The impregnated mass was dried in an air oven at 80 ºC overnight then, admitted into the reactor (ignition tube), which was then placed in a tubular electric furnace open from both ends. The temperature was raised at the rate of 50ºC/10 min. to the required end temperature. The carbonization process was carried out at temperature of 800 ºC for 1.5 hr. The product was thoroughly washed with hot distilled water, and finally dried at 110ºC [27-29]. and *second method* by $ZnCl_2$ ratio of 1:2 (O.S./ $ZnCl_2$) [30-32] The O.S mass was soaked in 150 mL of $ZnCl_2$ solution, then the same condition and steps as first method. Impregnation with $ZnCl_2$, first results in degradation of the cellulosic material and, on carbonization, produces dehydration that results in charring and aromatization of the carbon skeleton and creation of the pore structure [33].

2.3. Characterization of activated carbon:

The texture characteristics were determined by the standard N_2 adsorption isotherms, followed by their analysis to evaluate the porous parameters. Nitrogen adsorption isotherm was conducted at liquid nitrogen temperature using NOVA 1000e Quanta chrome. Surface area (SBET), mean pore diameter (d) and total pore volume (VP) were determined. The elemental analysis was measured by CHNS-O elemental analysis. The Physico chemical characterization of O.S carbon was summarized as Table (2)

Table 2: Physico chemical characterization of the studied Olive Stone sample.

Olive Stone sample	
Parameters	Values
C%	44.2
H%	1.9
N%	0.4
S%	0.04
O%	12.9
Lignin	30.5
Moisture	11.8
bulk	0.99

2.3. 1. Scanning Electron Microscope (SEM)

Morphology of sorbent beads was examined by scanning electron microscope (SEM) using QUANTA 200 with ≥10 kV accelerated voltage.

2.3. 2. Fourier Transform-Infrared spectroscopy (FTIR):

Infrared spectrum (FTIR) for the sorbent beads was examined using the mid-infrared region from 4000 cm^{-1} to 5000 cm^{-1} using FT-IR spectrometer (Bomen, Hartman & Braun, and model MB-157, Canada) under ambient air condition using KBr as a diluent.

2.4. Sorption methodology

Batch sorption experiments were performed by shaking 0.01 g of activated carbon with 15.0 mL of the commercial Wet-process phosphoric acid (WPA) in a thermostated shaker bath at (25 ± 1ºC), uranium ion of 50 ppm concentration; contact time of 180 min, After the corresponding time interval, the solutions were filtered through a 0.45 μm pore size membrane. Uranium concentration in the filtered solutions was determined using an inductively coupled plasma optical emission spectrometer (Optima 2100DV, Perkin-Elmer).

The amount of the uranium sorbed was calculated by the difference between the equilibrium concentration and the initial concentration. The amount of uranium retained in the solid phase qe (mg/g) was calculated using the following relation:

$$q_e = \left(C_o - C_e\right) \times \frac{V}{m} \qquad (1)$$

Where C_o and C_e are the initial and equilibrium concentrations (mg/L) of ions solution, respectively, V is the volume of solution (L) and m is the weight (g) of the adsorbent. The removal percent of ions from the aqueous phase is calculated from the following relation:

$$\text{Uranium adsorption \%} = \frac{C_o - C_e}{C_o} \times 100 \qquad (2)$$

The distribution coefficient (K_d) of uranium between the aqueous bulk phase and the solid phase was calculated from the following relation:

$$K_d = \frac{C_o - C_e}{C_o} \times \frac{V}{m} \qquad (3)$$

3. Results and discussion

3.1. Surface area of adsorbent:

The surface area and the porous structure of adsorbents were measured by N2 adsorption isotherm at 77 K using surface area and pore size analyzer where the obtained pore diameter was ≤0.003. The obtained data shows that BET constant value (c =3.5), which is related to the affinity of the solid with adsorbate**.** The value of c is the higher the interaction. Also, Figure 1 gives an indication that N2 adsorption isotherms of carbon Olive Stone are type I curve. The later depicts monolayer adsorption and this graph can be easily explained using Langmuir adsorption isotherm, then Type I Adsorption Isotherm is obtained. The BET surface area was 12.799e+00 m^2/g, total pore volume was1.34e-02 cc/g and radious of this material was 2.10e+01A° [34].

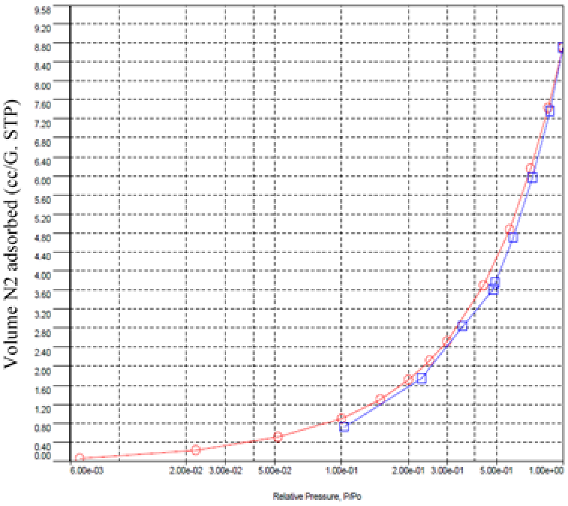

Fig (1): N_2 adsorption-de-sorption isotherms for the Olive Stone sample.

3.2. The Factors Effecting of Uranium Adsorption.

The influence of several parameters on the sorption behavior of the prepared carbon has been studied, by batch technique, in order to find out the preferred sorption conditions for uranium removal from Wet-process phosphoric acid. These parameters include shaking time (5-240 min), initial uranium ion concentration (50-600 ppm), acid concentration (10-44 %P_2O_5), and carbon amount (0.33-2 g/l).

3.2.1. Effect of carbon type:

The olive stone precursor was treated by different methods producing different types of activated carbon. The types of prepared activated carbon have a significant effect on the capacity of the sorption of U (VI) ion as shown in Table (3). The results obtained indicated that there is a high variation in the efficiency of some type of prepared activated carbon toward U (VI) ion. From the data obtained, it was found that olive stone impregnated with 50%H_3PO_4, heated to 800°C and 600°C $ZnCl_2$ ratio 1:2 carbonization temperature is the best one for sorption of the U (VI).

Table (3): Effect of carbon type on sorption (percent removal) of U (VI) ions.

Temperature, ◦C	O.S-$ZnCl_2$ %			O.S-H_3PO_4, %	Olive Stone%
	1/1	1/2	1/3		
400	45.56	68.22	70.2	46.19	15.55
500	55.8	76.5	75.9	55.50	25.28
600	60.62	➡ 85.91	86.33	83.64	30.81
800	41.14	86.21	86.64	➡ 92.55	32.7

3.2.2. Effect of contact time

The adsorption of U(VI) ions onto activated carbon was studied as a function of shaking time 15 mL of uranium solution 50 ppm (P_2O_5 : 44%) was shaking with 0.02g of activated carbon for different intervals of time ranging from 5 to 240 min. Figure 2 shows the variety of adsorption percentage of uranium with shaking time. during the first 180 min of the experiment, the concentration of U (VI) adsorbed on the activated carbon on two modifications O.S-$ZnCl_2$, O.S-H_3PO_4 increases from 20, 30% at 5 min. to 77, 87% at 180 min., respectively with the prolonged time. From 180 to 240 min, no high significant change of U (VI) concentration is observed. The results indicate that the adsorption equilibrium is reached after only 180 min. Similarly, the adsorption of U (VI) [35, 36] on the activated carbon also occurs quickly and 180 min are enough to achieve the adsorption equilibrium in O.S-H_3PO_4 and O.S-$ZnCl_2$.

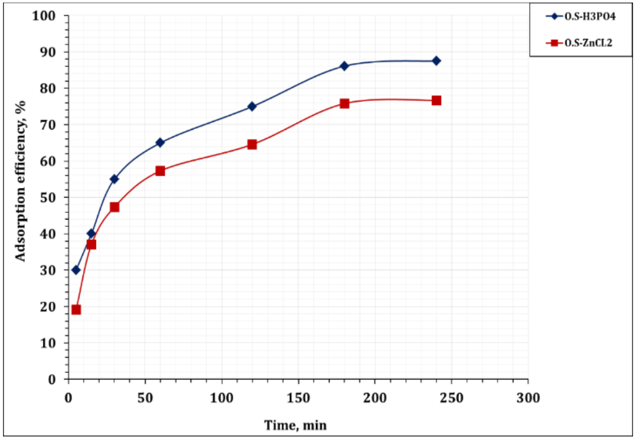

Fig (2): Effect of contact time on U (VI) adsorption onto O.S- H_3PO_4 and O.S-$ZnCl_2$. (15 mL of solution 50 ppm U (P_2O_5: 44%), 0.02g carbon, room temperature 25±1oC)

3.2.3. Effect of initial uranium concentration

The effect of uranium concentration was studied by using more than experimental different uranium-containing varying initial concentrations from 50 to 600 mg/L, at a fixed mass of activated carbon (0.02 g). Figure 3 shows that the removal efficiency of uranium decreases as the initial uranium concentration increases from 90, 80% at 50 mg/L to 10% at 600 mg/L respectively O.S-H_3PO_4 and O.S-$ZnCl_2$. This may be due to the fact that uranyl ions (UO_2^{2+}) in diluted solutions have higher mobility, so that interactions between ions and the adsorbent increase [37]. Maximum removal of uranium was observed at 50 mg/L uranium concentration.

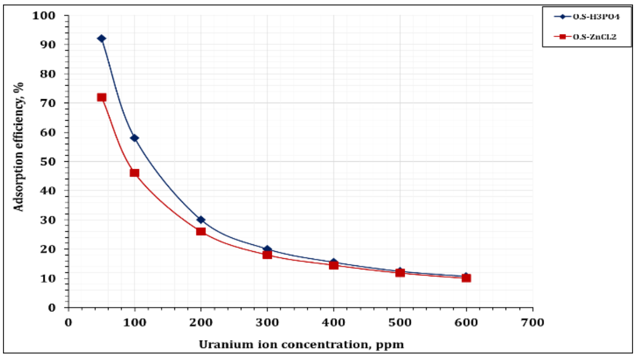

Fig (3): Effect of initial uranium concentration on U (VI) adsorption onto O.S- H_3PO_4 and O.S-$ZnCl_2$. (15 mL of solution (P_2O_5: 44%), 180 min., 0.02 g carbons, room temperature 25±1oC)

3.2.4. Effect of phosphoric acid concentration

The effect of phosphoric acid concentration is the most important parameter for the adsorption experiments. In this study, the acid concentrations were varied between 10% and 44%, keeping the other parameters constant, shaking time 15 mL of uranium solution 50 ppm was shaking with 0.02 g of activated carbon for 180 min. Figure 4 shows the effect of phosphoric acid concentration on the adsorption of U (VI) ions onto activated carbon by two modifications O.S-H_3PO_4, O.S-$ZnCl_2$. The percentage of adsorption slight decreases with increasing phosphoric acid concentration from 90 to 80%. The effect of phosphoric acid concentration on uranium adsorption can be explained in the following way: increasing P_2O_5 concentration is associated with the increase of hydrogen protons in the solution which can compete uranium adsorption on the surfaces of carbon particles [38].

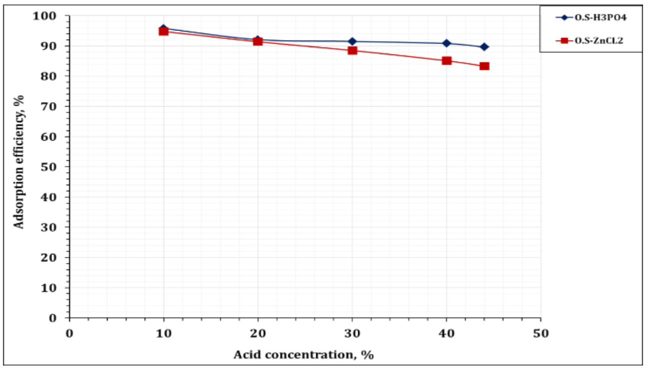

Fig (4): Effect of phosphoric acid concentration on U (VI) adsorption onto O.S- H_3PO_4 and O.S-$ZnCl_2$. (15 mL of solution 50 ppm U ,180 min., 0.02g carbon, room temperature 25±1°C)

3.2.5. Effect of the temperature

The effect of temperature on the sorption of uranium ions from phosphoric acid by O.S-H_3PO_4 and O.S-$ZnCl_2$ was studied in the range 25–60 ±1°C. The other parameters were fixed at uranium initial concentration of 50 mg/ L, sorbent amount of addition of 0.02 g/ 15 mL, and contact time of 180 min. From the results shown in Figure 5, it is clear that increasing the temperature from 25–60°C leads to decrease the adsorption percent from 90% to 40% for O.S-H_3PO_4 and from 83% to 26% for O.S-$ZnCl_2$. This behavior indicates that the uranium sorption process by O.S-H_3PO_4 and O.S-$ZnCl_2$ is an exothermic process. Room temperature will be the chosen temperature for the other sorption investigation.

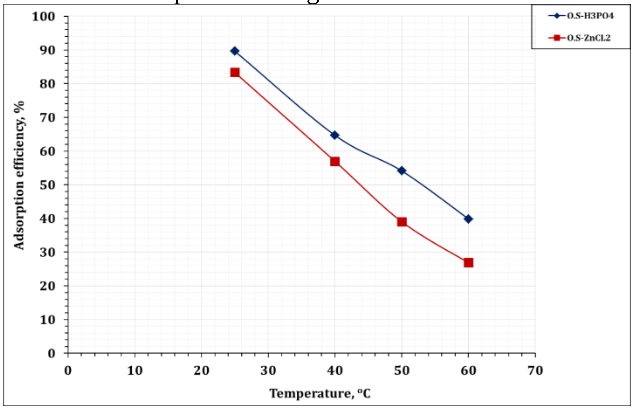

Fig (5): Effect of Temperature on U (VI) adsorption onto O.S- H_3PO_4 and O.S-$ZnCl_2$. (15 mL of solution 50 ppm U (P_2O_5: 44%), 0.02g carbon, 180 min.)

3.2.6. Effect of Adsorbent Weight

Sorption efficiency as a function of Adsorbent amount (0.33-2 g/L) was executed on uranium ion of 50 ppm concentration; contact time of 180 min, and reaction temperature of 25 ±1°C. The experimental data was shown in Figure 6. The results revealed that the sorption efficiency is directly related to the Adsorbent amount, i.e. it increases with increasing Adsorbent amount. The maximum sorption efficiencies reached 90% and 83% for O.S-H_3PO_4 and O.S-$ZnCl_2$, respectively in amount 1.33g/L, when 1.33 g/ L of each modification was used. This was attributed to increasing the number of binding sites available to catch uranium ion [39-41]. Further increase in the Adsorbent amount of addition up to 2 g/ L has slight effect on the uranium sorption efficiency.

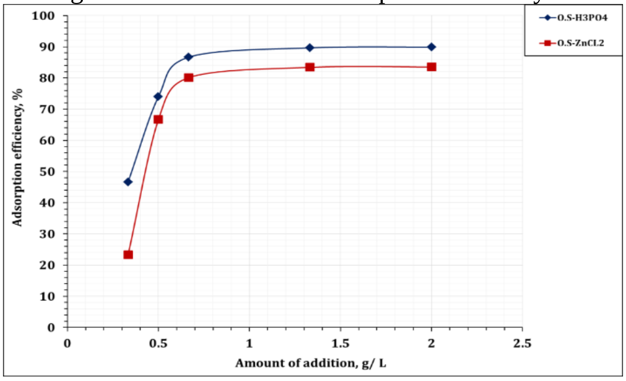

Fig (6): Effect of Adsorbent Weight on U (VI) adsorption onto O.S-H_3PO_4 and O.S-$ZnCl_2$. (15 mL of solution 50 ppm U (P_2O_5: 44%), 180 min., room temperature 25±1oC)

3.3. Sorption isotherms studies

Sorption isotherm describes an equilibrium state between the sorbent and the sorbate at constant temperature. Equilibrium isotherms are used to determine the capacity of adsorbents for metal ions. Several isotherm models were reported, of which two different sorption isotherms namely Langmuir and Freundlich were considered to fit the experimental data obtained during the current study.

Freundlich isotherm

Freundlich equation is derived to model the. The Freundlich isotherm can be used for the multilayer sorption and for the sorption on heterogeneous surfaces and is expressed by the following equation [42]:

$$qe = Kf\ C1/n \qquad (4)$$

A linear form was obtained by taking logarithms to find the parameters Kf and n:

$$\log qe = \log Kf + (1/n) \log Ce \qquad (5)$$

where Kf and (1/n) are constants that indicate sorption capacity (mg/g) and sorption intensity, respectively, and are obtained by plotting log qe vs. log Ce, Figure 7a and Table 4).

Langmuir isotherm

The Langmuir adsorption model is based on the assumption that maximum adsorption corresponds to a saturated monolayer of solute molecules on the adsorbent surface. The Langmuir equation can be described as the following [43]:

$$Ce/qe = 1/Q0b + Ce/Q0 \qquad (6)$$

where qe is the amount of sorption per unit mass of polymer at equilibrium (mg/g), Ce is the equilibrium concentration of the solute in the bulk solution (mg/L), Qo is the monolayer adsorption capacity (mg/g) and b is the Langmuir constant, which can be considered as a measure of sorption energy.

The obedience of the sorption process to Langmuir isotherm model was confirmed by the linear plot, with R2 = 0.99, obtained when (Ce/qe) was plotted against Ce (Figure 7b). The numerical value of constants Qo and b evaluated from the slope and intercept of the straight lines (Figure 7b).

The maximum uptake amounts of U (VI) obtained experimentally, 47.85 and 46.08 mg/g for O.S-H_3PO_4 and O.S-$ZnCl_2$, respectively, were of a good agreement with the theoretical values calculated from the isotherm studies, Table 4.

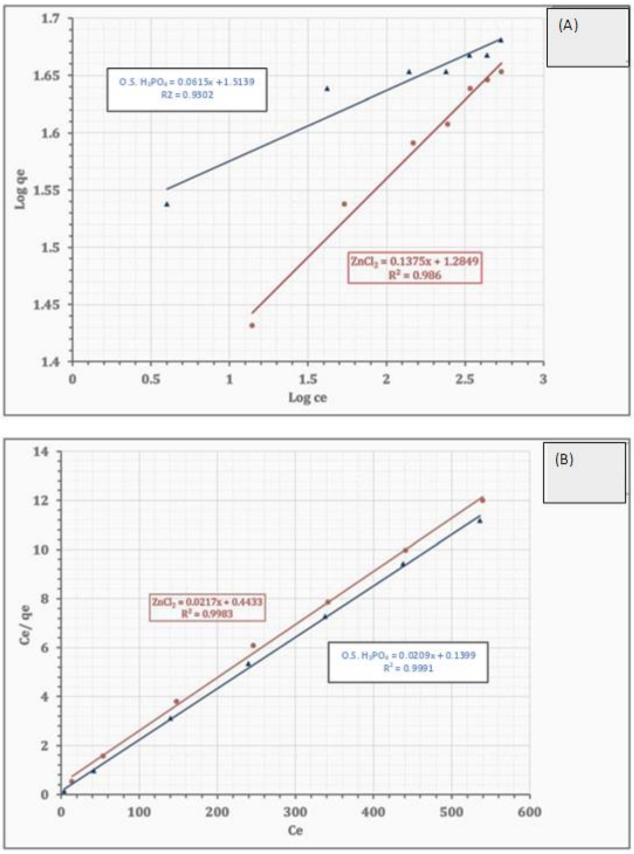

Fig (7): (a) Freundlich and (b) Langmuir isotherm plots for sorption of uranium ion on O.S-H_3PO_4 and O.S-$ZnCl_2$

Table 4: Freundlich and Langmuir isotherm parameters for the sorption of uranium on O.S-H_3PO_4 and O.S-$ZnCl_2$.

			O.S-H_3PO_4	O.S-$ZnCl_2$
Freundlich isotherm model	Kf (mg/ g)		32.65	19.27
	n		16.26	7.27
	R^2		0.93	0.98
Langmuir isotherm model	Qm (mg/g)		47.85	46.08
	b (L/ mg)		0.149	0.049
	R^2		0.99	0.99
	RL	Co	O.S-H_3PO_4	O.S-$ZnCl_2$
		50	0.118	0.290
		100	0.063	0.170
		200	0.032	0.093
		300	0.022	0.064
		400	0.016	0.049
		500	0.013	0.039
		600	0.011	0.033

A comparison of the adsorption capacity of O.S- H_3PO_4 and O.S-$ZnCl_2$ with some other sorbents is provided in (Table 5).

Table 5: The experimental capacity of O.S- H_3PO_4 and O.S-$ZnCl_2$ compared with the sorption capacity of some other sorbents:

Type	sorption capacity, (mg/ g)	Ref.
polyethyl eniminephenyl phosphonamidic acid	39.6	[44]
succinic acid impregnated amberlite XAD-4	12.3	[45]
gel-amide	28.9	[46]
gel-benzamide	18.6	[47]
natural clinoptilolite zeolite	0.7	[48]
O.S-H_3PO_4 Activated Carbon	47.85	Present work
O.S-$ZnCl_2$ Activated Carbon	46.08	

3.4. Kinetic studies

Two kinetic models, namely pseudo-first order and pseudo second order, were applied to the experimental data to investigate the mechanism of the sorption process. The linear form of pseudo-first order equation is given as [49]:

$$\text{Log}\,(q_e - q_t) = \text{Log}\, q_e - \frac{K_2}{2.303}\,\text{t} \qquad (7)$$

where qt is the sorption capacity at time t (mg/g), qe is the sorption capacity at equilibrium (mg/g) and K1 is the rate constant of the pseudo-first-order sorption (1/min). From the slope and intercept of the linear interpolation of Log (qe-qt) versus t (Figure 8a) the values of K1 and qe as well as R2 were determined and listed in Table 6. The R2 values obtained from the pseudo first-order kinetic plots are good enough to assume the fitting of the sorption process to this kinetic model. However, the calculated qe values do not match the experimental values for the sorption process (Table 6). Thus, the pseudo first-order model was excluded.

In the pseudo-second order, the model assumes that the adsorption capacity is proportional to the number of active sites on the surface of the absorbent. The linear form of pseudo-second order equation is expressed as follows [50]:

$$\left(\frac{t}{q_t}\right) = \frac{1}{K_2 q_e^2} + \frac{1}{q_e}\,\text{t} \qquad (8)$$

K2 is the rate constant of the pseudo-second-order kinetics (g/mg min). Moreover, the initial sorption rate (h) (mg/g min) can be calculated by usage of the following equation:

$$\text{h} = K_2 q_e^2 \qquad (9)$$

The values of K2, qe and h were calculated from the slope and intercept of the straight lines obtained when t/qt was plotted against t (Figure 8b) and were given in Table 6. As presented in Table 6, for the pseudo-second order kinetic model, the obtained correlation coefficients, R2 values were higher than 0.99 and the values of qe,exp from the experimental data were very close to the calculated qe values. Therefore, the sorption process of U(VI) ion on O.S- H_3PO_4, O.S-$ZnCl_2$ is said to follow the pseudo-second order kinetic model. This means that, the overall sorption process is dependent on the amount of uranium ions which exist in solution and the number of active sites on O.S-H_3PO_4 and O.S-$ZnCl_2$.

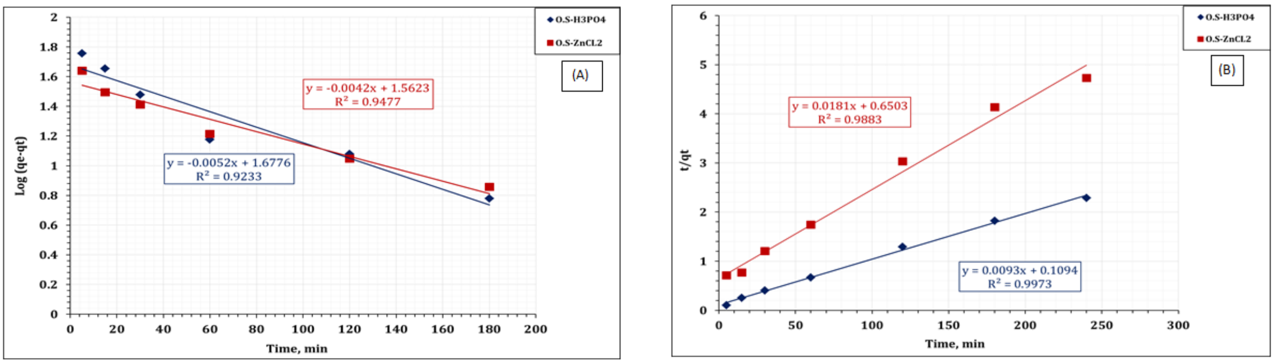

Fig (8): Pseudo first order (a) and pseudo second-order (b) plots for the sorption of uranium using O.S-H_3PO_4 and O.S-$ZnCL_2$.

Table (6): The calculated parameters of the pseudo first-order and pseudo second-order kinetic models for adsorption of uranium by using O.S-H_3PO_4, O.S-$ZnCl_2$.

	Lagergreen pseudo first-order				pseudo second-order			
	K_1 (min $^{-1}$)	qe_{cal} (mg/ g)	qe_{exp} (mg/ g)	R^2	K_2 (min $^{-1}$)	qe_{cal} (mg/ g)	qe_{exp} (mg/ g)	R^2
O.S- H_3PO_4	0.022	65.3	105.0	0.92	0.0007	111.1	105.0	0.99
O.S-$ZnCl_2$	0.021	77.9	92.0	0.94	0.0005	99.0	92.0	0.98

3.5. Thermodynamic studies

The van't Hoff relation [51] can be used to calculate the enthalpy changes associated with the adsorption process of uranium (VI) ions from Egyptian phosphoric acid by O.S-H_3PO_4 and O.S-$ZnCl_2$.

$$\log K_d = -\frac{\Delta H}{2.303\, R} \text{ X } \frac{1}{T} + \text{C} \qquad (10)$$

where R is the universal gas constant, and C is a constant.

From the plot of log K_d versus (1/ T) Figure 9, a straight line was observed, from which ΔH (the enthalpy change) can be calculated.

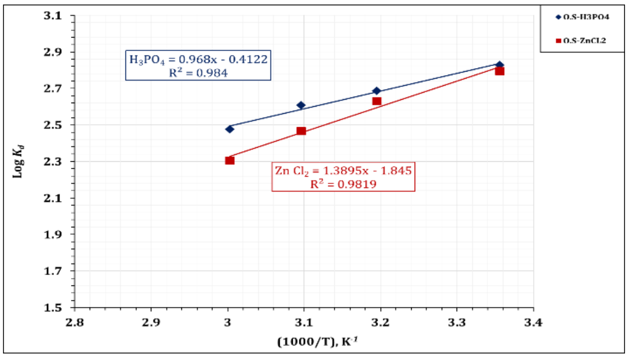

Fig (9): Variation of log K_d with 1/T for uranium adsorption by O.S-H_3PO_4 and O.S-$ZnCl_2$

The Gibbs free energy change, Δ G was also calculated based on the logarithmic value of the distribution ratio Log K_d at 20 ± 1 °C according to the following equation:

$$-\Delta \text{G} = 2.303 \text{ RT} \log K_d \qquad (11)$$

Also, the entropy change, ΔS was obtained from ΔG and ΔH with the following equation:

$$\Delta \text{G} = \Delta \text{H} - \text{T}\, \Delta \text{S} \qquad (12)$$

The thermodynamic parameters of the adsorption of uranium (VI) ions by O.S-H_3PO_4 and O.S $ZnCl_2$ are given in Table 7 ,where ΔH, ΔG, (kJ mol^{-1}) and ΔS (J mol^{-1} K^{-1}).

Table 7: Thermodynamic parameters for uranium adsorption using O.S-H_3PO_4 and O.S-$ZnCl_2$

	ΔH	ΔG	ΔS
O.S- H_3PO_4	-18.534	-16.133	-8.06004
O.S-$ZnCl_2$	-26.605	-15.952	-35.7486

The magnitude and sign of the enthalpy change (ΔH) associated with the sorption process will consist of: (1) enthalpy change for dehydration (ΔH_d) which can be expected to be positive because energy is required to break the ion–water and water–water bonding of the hydrated metal ions, and (2) enthalpy change for complexing (ΔH_c) which will make ΔH more negative due to the formation of metal complex [52]. While the negative sign of the free energy change value indicated the spontaneous phenomenon of uranium (VI) ions adsorption and the value sign of the entropy variation suggested that the system exhibit a disorder.

3.6. Uranium elution:

Uranium elution from the loaded O.S-H_3PO_4 and O.S-$ZnCl_2$ has been investigated using the following solutions; H_2SO_4, HNO_3, HCl, and Na_2CO_3. Desorption experiments were carried out by shaking the loaded O.S-H_3PO_4 and O.S-$ZnCl_2$ sample (0.05 g) with 25 mL of the eluent solution (0.1 M). The elution efficiency has been calculated systematically and presented in Table 8. The obtained date shows that HNO_3 solution is the preferred for uranium elution from the loaded O.S-H_3PO_4 and O.S-$ZnCl_2$

Table 8: Uranium desorption from loaded O.S-H_3PO_4 and O.S-$ZnCl_2$ by different solutions.

Eluent solution	Efficiency, %	
	O.S-H_3PO_4	O.S-$ZnCl_2$
0.1 M H_2SO_4	54.1	64.4
0.1 M HNO_3	75.4	82.8
0.1 M HCl	41.9	57.3
0.1 M Na_2CO_3	25.2	38.9

3.7. Characterization of adsorption

3.7. 1. Scanning electron microscope:

Scanning electron microscope has been utilized to detect the change in adsorbent (carbon) morphology before and after uranium sorption. The SEM photographs of O.S-H_3PO_4 and O.S-$ZnCl_2$ surface cross section before and after the sorption of uranium (VI). Analysis of SEM images revealed that structure before the sorption of uranium Figure 10 (A, B) respectively has been changed by uranium capture. Additionally, the pores were changed after U (VI) sorption Figure 10(C, D) respectively which emphasizes the filling of such pores by U (VI) due to intermolecular interaction.

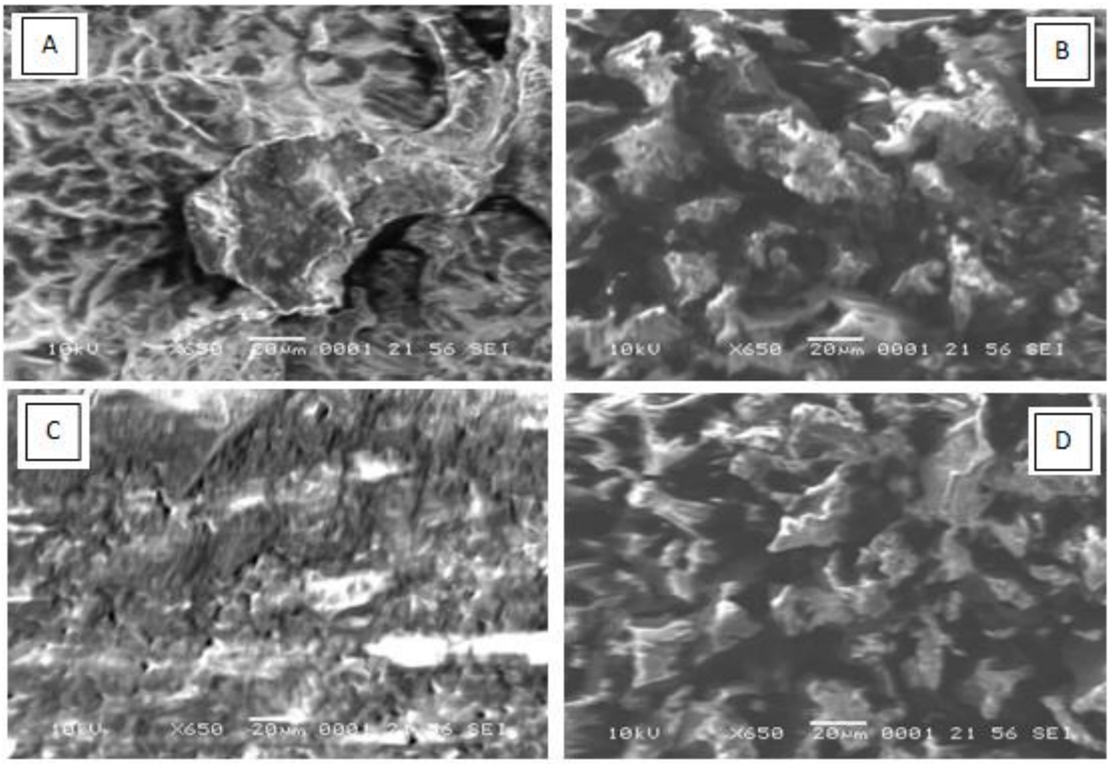

Fig (10): SEM images for O.S-H_3PO_4 and O.S-$ZnCL_2$ (A and B) before and (C and D) after sorption of uranium (VI), respectively.

3.7. 2. FTIR spectroscopy:

The infrared spectra of adsorbents were obtained from a Fourier Transform Infrared Spectrophotometer (FTIR) using the KBr disc. The loading capacity of carbon derived from olive stone depends on the porosity, pore content and functional group reactivity on the surface. IR spectrum was used to qualitatively interpret the functional groups on the carbon modification.

The carbon showed the broad bands at 3500 and 1081 cm^{-1} which may be due to hydrogen bonded -OH and P-O. Thus, the surface OH groups probably interact with water molecules adsorbed by the carbon samples from the environment. (Figure11). Carbons OS, O.S-H_3PO_4 and O.S-H_3PO_4 loaded U show an absorption band at 1384 cm^{-1} which may be due to -NH bending. The shoulders at 3600 and 2300 cm^{-1} denote the presence of asymmetric and symmetric stretching C-H vibrations of CH_3 group. The bands at 1019 and 1314 cm^{-1} in O.S-H_3PO_4 and O.S-H_3PO_4 loaded U may be due to the stretching P-OH or S-O stretching vibrations and P-S stretching respectively.

Comparison of the spectra shows that the intense bands at 1625 cm^{-1}, which could indicate a greater concentration of COO- or to skeletal C-C aromatic vibrations and the band at 1077 cm-1, may be due to phenolic OH groups in the sorbent *O.S-H_3PO_4* as a result of greater oxidation of the carbon surface by air at 800◦C. Some of bands disappear due to the chemical reaction which happened between adsorbate and adsorbent. (Figure12). Carbons OS, O.S-$ZnCL_2$ and O.S-$ZnCl_2$ loaded U show an absorption band at 1384 cm^{-1} which may be due to -NH bending. The shoulders at 3676 and 3419 cm^{-1} denote the presence of asymmetric and symmetric stretching C-H vibrations of CH_3 group. the stretching band at 3439 cm_1 is ascertained to the hydroxyl group. The bands at 1019 O.S-$ZnCL_2$ due to the stretching P-OH. The absorption bands stretching at 3600 cm^{-1} modes and 1011 cm^{-1} became wider, which change significantly before and after uranium adsorption (Figure 13).

]

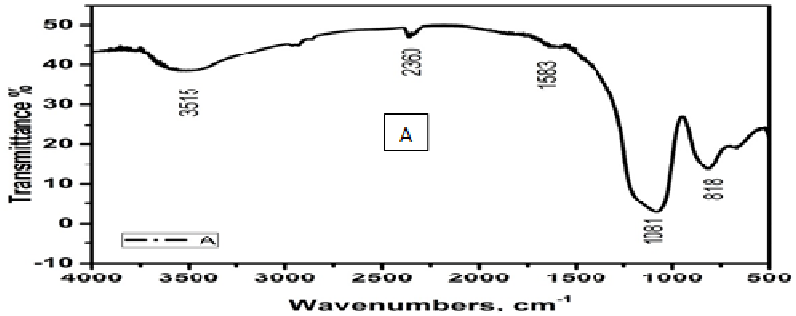

Fig (11): FTIR spectra of the plank olive stone carbon (O.S.) (A).

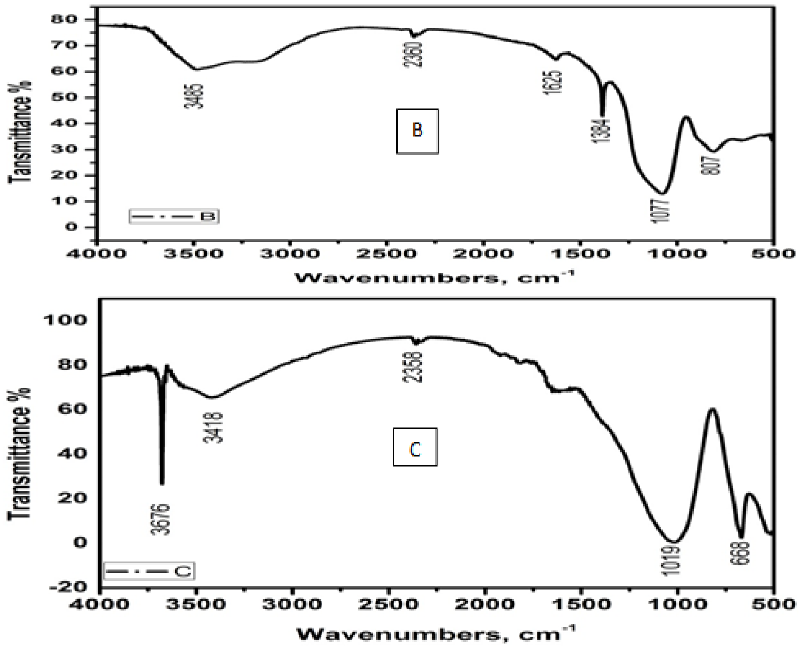

Fig (12): FTIR spectra of olive stone activated carbon by phosphoric acid before uranium adsorption (O.S-H_3PO_4) (B) and after uranium adsorption (C).

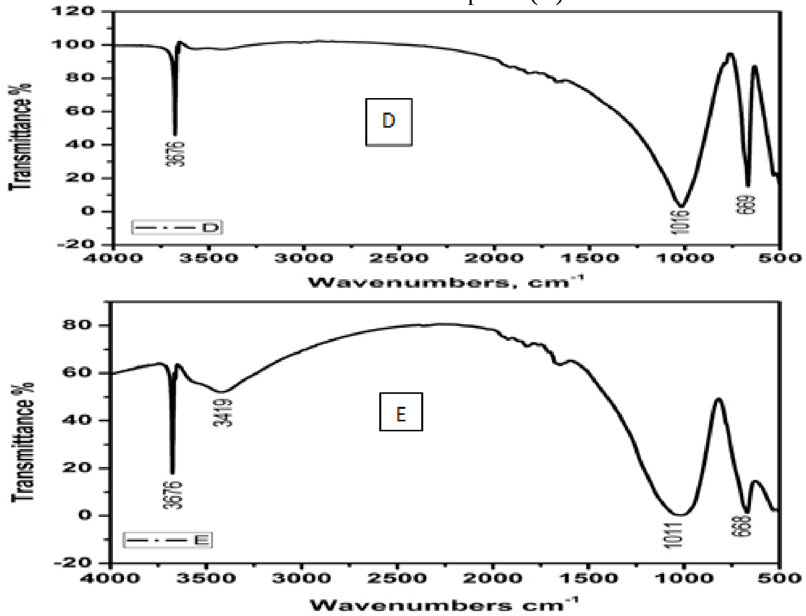

Fig (13): FTIR spectra of olive stone activated carbon by $ZnCL_2$ (O.S-$ZnCL_2$) (D) before uranium sorption and (E), after uranium adsorption.

4. Conclusion

The obtained data reflects the possibility of recovery uranium U(VI) from Egyptian crude phosphoric acid using O.S-H_3PO_4 and O.S-$ZnCl_2$ and H_2O_2 must be added to the phosphoric acid before applying the uranium adsorption process. Not less than 90% and 83% for O.S-H_3PO_4 and O.S-$ZnCl_2$, respectively at the optimum adsorption conditions of concentration of 44% of P_2O_5, U (VI) concentration of 50 mg/L, stirring time of 180 min, amount of carbon 1.33g/L at room temperature. The maximum sorption capacity about 48 mg/g and 46 mg/g for O.S-H_3PO_4 and O.S-$ZnCl_2$, respectively of U(VI). The adsorbed uranium U(VI) was already desorbed by stirring with 0.1 M HNO_3 for 30 min for desorbing 80% of uranium from loaded O.S-H_3PO_4 and O.S-$ZnCl_2$ carbon.

Acknowledgement

The author would like to express his sincere thanks to ***Associate Prof. Dr. M. H. Taha*** *and* ***Associate Prof. Dr. A. E. M. Hussein*** for deeply useful scientific discussions during performing this paper.

References

[1] T.S. Anirudhan, P.G. Radhakrishnan, "Improved performance of a biomaterial-based cation exchanger for the adsorption of uranium (VI) from water and nuclear industry wastewater ", J. Environ. Radioact. 100 (2009) 250-257.

[2] W. Zou, L. Zhao, R. Han, " Removal of uranium (VI) by fixed bed ion-exchange column using natural zeolite coated with manganese oxide ", Chin. J. Chem. Eng. 17 (2009) 585-593.

[3] European Fertilizer Manufacturers Association, "Production of phosphoric acid", Booklet No. 4 of 8, (2000). Belgium.

[4] M. M. Ali a, A. E. M. Husseina, W. M. Youseif a and A.M. El Didamony, "Application of Solvent-In-Pulp Technique for Uranium Extraction from Mineralization Granite" Arab Journal of Nuclear Sciences and Applications, 50 (2017) 217-228.

[5] A. E. M. Hussein, W. M. Youssef, M. H. Taha and M. M. El-Maadawy, "Uranium Adsorption from Aqueous Nitric Acid Solution by Solvent Impregnated Polypropylene" Arab Journal of Nuclear Sciences and Applications, 50 (2017) 156-170

[6] W.M. Youssef, "Uranium Adsorption from Aqueous Solution Using Sodium Bentonite Activated Clay" J. Chem. Eng. Process Technol. 8 (2017) 1-3.

[7] W. M. Youssef, M. S. Hagag and A. H. Ali, "Synthesis, characterization and application of composite derived from rice husk ash with aluminum oxide for sorption of uranium" Adsorption Science & Technology, (2018) 1–20

[8] A.M.A. Morsy, A.E. M. Husien and W. M. Youssef, "Adsorption Features of Uranium ions from Aqueous Solutions by Poly Vinyl Alcohol/Poly Aniline Composite" J. Bas. & Env. Sci., 4 (2017) 329-338

[9] A. Leydiera., G. Arracharta, R.Turgisa, Bernierb G., Marieb C., M. Miguirditchianb, Pellet-Rostainga S., "Recovery of uranium (VI) from concentrated phosphoric acid using bifunctional reagents, Hydrometallurgy" 171 (2017) 262–266.

[10] W. M. Youssef, "Studies on The Recovery of Uranium from Gattar And Sella Mineralization By Solvent-In-Pulp Technique". A Thesis Sumitted to the Faculty of Science, Zagazig University, phd, (2014)

[11] A. Charlot, S. El. Mourabit, F. Goettmann, Arrachart G. Turgisb R. Grandjean, "From phosphate rocks to uranium raw materials: hybrid materials designed for selective separation of uranium from phosphoric acid." RSC Adv. 4 (109), (2014) 64138–64141.

[12] J. McKinley, Z. Smith., G.Turner, "The influence of uranyl hydrolysis and multiple site-binding reactions on adsorption of U(VI) to montmorillonite" Clays and Clay Minerals 43 (1995) 586 – 598.

[13] D.Guerra, V Leidens., R.Viana, C.Airoldi, "Amazon kaolinite functionalized with diethylenetriamine moieties for U (VI) removal: thermodynamic of cation-basic interactions" Journal of Hazardous Materials 180 (2010) 683 – 692.

[14] S. Aytas, S. Akyil, M. Eral, "Adsorption and thermodynamic behaviour of uranium on zeolite" Journal of Radioanalytical and Nuclear Chemistry 260 (2004) 119 – 125.

[15] M. Bonato, K.Ragnarsdottir, G.Allen, "Removal of uranium (VI), lead (II) at the surface of TiO2 nanotubes studied by X-ray photoelectron spectroscopy" Water Air Soil Pollut. 223 (2012) 3845 – 3857.

[16] ZZ Chowdhury SM, Zain, RA Khan, S Islam. "Preparation and characterizations of activated carbon from kenaf fiber for equilibrium adsorption studies of copper from wastewater". J. Applied Sciences Engineering and Technology, 29 (2012) 1187-1195.

[17] T Dula, K Siraj, SA Kitte. "Adsorption of Hexavalent Chromium from Aqueous Solution Using Chemically Activated Carbon Prepared from Locally Available Waste of Bamboo (Oxytenanthera abyssinica)" ISRN Environmental Chemistry (2014).

[18] M Danish, R Hashim, MNM Ibrahim, O Sulaiman. "Effect of acidic activating agents on surface area and surface functional groups of activated carbons produced from Acacia mangium wood" J Anal Appl Pyrolysis.;104: (2013), 418-425.

[19] H. A Salmani, "Comparative study of copper (ii) removal on iron oxide, aluminum oxide and activated carbon by continuous down flow method" J Toxicol Environ Heal Sci., 5 (2013) 150-155.

[20] MA Nahil, PT Williams. Pore characteristics of activated carbons from the phosphoric acid chemical activation of cotton stalks. Biomass and Bioenergy. 37: (2012); 142-149. doi:10.1016/j. biombioe. 2011.12.019.

[21] H Almana, R Mahmoud "Palm Date Seeds as an Alternative Source of Dietary Fiber in Saudi Bread", Ecol. Food Nutr., Vol. 32 (1994) pp. 261-270.

[22] A; Gierak, F Czechowski.; A Leboda.. “Improvement of Carbon-silica Adsorbent (carbosil) Surface Properties Upon Steam Activation at 1073 K”, Mater Chem Phys., Vol. 36 (1994) pp. 264-270.

[23] C. Kirubakaran, S. Krishnaiah, S.Seshdri, “Experimental Study of the Production of Activated Carbon from Coconut Shells in a Fluidized Bed Reactor”, Ind. Eng. Chem. Res.,Vol. 30, (1991), pp. 2411-2416.

[24] Z. Guo, Z Yan., Z.Tao “Sorption of uranyl ions on TiO2: effects of contact time, ionic strength, concentration and humic substance” Journal of Radioanalytical and Nuclear Chemistry 261 (2004) 157 – 162.

[25] G. Drisko, M. Chee, N. Scales, A. Ide, E. Sizgek, R. Caruso, V. Luca “One-pot preparation and uranyl adsorption properties of hierarchically porous zirconium titanium oxide beads using phase separation processes to vary macropore morphology, Langmuir 26 (2010) 17581 – 17588.

[26] G. Rodríguez, A. Lama, R. Rodríguez, A. Jiménez, R. Guillén and J. Fernández-Bolaños “Olive stone an attractive source of bioactive and valuable compounds, Bioresource Technology” 99 (2008) 5261-5269.

[27] H.M.H. Gad, M. M. S. Ali, W. F. Zaher, E.A. El-Sofany,S.A.Abo-El-Enein “Application of Olive Stone Based Activated Carbon in the Sorption of Lanthanum (III) Ions from Aqueous Solution” Arab Journal of Nuclear Science and Applications, 47 (2014) 67-79

[28] H. M. H. Gad, S. I. El-Dessouky** & A. A. M. Daifullah “A Study of the Factors Affecting the Removal of Lanthanides from Nitrate Solution by Activated Carbon Prepared from Date Pits” International Journal of Environmental Engineering Science volume 2 f number 1 f january-june, (2011) F 29-50

[29] C. Kutahyah, M.Eral, Y.Altas, H.Tel, Adsorption Of Uranium From Aqueous Solutions Using Activated Carbon Prepared From Olive Stones, Proceedings of the Third Eurasian Conference "Nuclear Science and its Application" (2004) 5-8.

[30] T. Budinova, E. Ekinci, F. Yardim, A. Grimm, E. Björnbom, V. Minkova and M. Goranova, “Characterization and application of activated carbon produced by H3PO4 and water vapor activation” Fuel Processing Technology, 87 (2006) 899-905.

[31] M. Ugurlu, A. Gurses and M. Acıkyıldız, Comparison of textile dyeing effluent adsorption on commercial activated carbon and activated carbon prepared from olive stone by ZnCl2 activation, Microporous and Mesoporous Materials, 111, (2008), 228-235.

[32] H. N. I. Nassar M.SC., “Nitrate and Nitrite Ion Removal from Aqueous Solutions by Activated Carbon Prepared from Olive Stones” An-Najah National University, Faculty of Graduate Studies, (2012)

[33] M. Smisek and S. Cerny “Active carbon: Manufucture, properties and applications” Elsevier, Amsterdam (1970).

[34] J. A. Alburquerque, J. Gonz_alvez, D. Garcıa, and J. Cegarra “Agrochemical characterisation of ‘‘alperujo’’ a solid by-product of the two-phase centrifugation method for olive oil extraction” Bioresource Technology, 91 (2004) 195-200.

[35] T. T. Al-Khalid, N. M. Haimour, S. A. Sayed and B. A. Akash “Activation of olive-seed waste residue using CO2 in a fluidized-bed reactor” Fuel Processing Technology, 57 (1998) 55-64.

[36] R. Yavuz, H. Akyildiz, N. Karatepe and E. Çetinkaya “Influence of preparation conditions on porous structures of olive stone activated by H3PO4” Fuel Processing Technology, 91, (2010), 80-87.

[37] C. Moreno-Castilla, F. Carrasco-Marı n, M. V. López-Ramón and M.A. Alvarez-Merino “Chemical and physical activation of olive-mill waste water to produce activated carbons” Carbon, 39 (2001) 1415-1420.

[38] A. El-Hamouz, H. S. Hilal, N. Nassar and Z. Mardawi, Solid olive waste in environmental cleanup:Oil recovery and carbon production for water purification, J. Environmental Management, 84 (2007), 83-92.

[39] Z.Yi, , J.Yao, , Y.Kuang, , H.Chen, , Wang, F., Xu, J.: “Uptake of hexavalent uranium from aqueous solutions using coconut husk activated carbon” Desalin. Water Treat 57 (2016) 1749

[40] C Kutahyali, M Eral “Selective adsorption of uranium from aqueous solutions using activated carbon prepared from charcoal by chemical activation” Sep Purif Technol 40 (2004) 109–114

[41] A.E.M.Hussein وA.M.A.Morsy “Uranium recovery from wet-process phosphoric acid by a commercial ceramic product” Arabian Journal of Chemistry 10 (2017) S361-S367

[42] P. Zong, H. Wang, H. Pan, Y. Zhao, C. “He, Application of NKF-6 zeolite for the removal of U(VI) from aqueous solution” J. Radioanal. Nucl. Chem. 295 (2013) 1969-1979.

[43] TM Uddin, SM Islam, ZM Abedin “Adsorption of Phenol from Aqueous Solution by Water Hyacinth Ash” Arpn J. Eng. Appl. Sci., 2 (2007) 11-17.

[44] L., Li, D., Ding, N., Hu, P., Fu, X., Xin, Y., Wang, “Adsorption of U(VI) ions from low concentration uranium solution by thermally activated sodium feldspar” J. Radioanal Nucl Chem 299 (2014) 681–690.

[45] O. Abderrahim, M.A., Didi, D. Villemin “A new sorbent for uranium extraction polyethyl enamine phenyl phosphon amidic acid” J. Radioanal Nucl Chem 279: (2009) 237–244.

[46] P., Metildaa, K., Sanghamitrab, J., Mary Gladisa, G.R.K., Naidub, T., Prasada Rao, “Amberlite XAD-4 functionalized with succinic acid for the solid phase extractive preconcentration and separation of uranium (VI)” Talanta 65 (2005) 192–200.

[47] K. A., Venkatesan, V., Sukumaran, M. P., Antony, P. R., Vasudeva Rao “Extraction of uranium by amine, amide and benzamide grafted covalently on silica gel” J. Radioanal Nucl Chem 260 (2004) 443–450.

[48] L.M., Camacho, S., Deng, R.R., Parra, “Uranium removal from groundwater by natural clinoptilolite zeolite: effects of pH and initial feed concentration” J Hazard Mater 175 (2010):393–398.

[49] Y.S. Ho, G. McKay “Pseudo-second order model for sorption processes” Process Biochem. 34 (1999) 451-465.

[50] T. G. Srinivasan, P. R. V. Rao, D. D. Sood “The Effect of Temperature on the Extraction of U (VI) from

Nitric Acid by Tri-n-Amyl Phosphate" Solvent Extraction and Ion Exchange 15 (1997) 15-31.
[51] H. Zhang, Y.Xie, Z.Tao, "Sorption of uranyl ions on gibbsite: effects of contact time, pH, ionic strength, concentration and anion of electrolyte" Colloids and Surfaces A: Physicochem. Eng. Aspects 252 (2005) 1–5.
[52] W. Cheng, C. Ding, Q Wu, X Wang, Y Sun, W Shi, T Hayat, A Alsaedi, Chaic Z, Wang X, "Mutual effect of U(VI) and Sr(II) on graphene oxides: evidence from EXAFS and theoretical calculations" Environmental Science: Nano 4 (2017) 1124–1131.